



**GIS and RS
techniques – land
use changes impact
on flood hydrology**

D. D. Alexakis et al.

GIS and remote sensing techniques for the assessment of land use changes impact on flood hydrology: the case study of Yialias Basin in Cyprus

D. D. Alexakis¹, M. G. Gryllakis², A. G. Koutroulis², A. Agapiou¹,
K. Themistocleous¹, I. K. Tsanis², S. Michaelides³, S. Pashiardis³,
C. Demetriou⁴, K. Aristeidou⁴, A. Retalis⁵, F. Tymvios³, and D. G. Hadjimitsis¹

¹Cyprus University of Technology, Dept. of Civil Engineering and Geomatics,
Remote Sensing and Geo-Environment Lab, Limassol, Cyprus

²Technical University of Crete, Dept. of Environmental Engineering, Chania, Crete, Greece

³Cyprus Meteorological Service, Nicosia, Cyprus

⁴Water Development Department, Nicosia, Cyprus

⁵National Observatory of Athens, Athens, Greece

Received: 7 July 2013 – Accepted: 25 July 2013 – Published: 13 September 2013

Correspondence to: D. D. Alexakis (dimitrios.alexakis@cut.ac.cy)

Published by Copernicus Publications on behalf of the European Geosciences Union.

Title Page	
Abstract	Introduction
Conclusions	References
Tables	Figures
⏪	⏩
◀	▶
Back	Close
Full Screen / Esc	
Printer-friendly Version	
Interactive Discussion	



Abstract

Flooding is one of the most common natural disasters worldwide, leading to economic losses and loss of human lives. This paper highlights the hydrological effects of multi-temporal land use changes in flood hazard within the Yialias catchment area, located in central Cyprus. Calibrated hydrological and hydraulic models were used to describe the hydrological processes and internal basin dynamics of the three major sub-basins, in order to study the diachronic effects of land use changes. For the implementation of the hydrological model, land use, soil and hydrometeorological data were incorporated. The climatic and stream flow data were derived from rain and flow gauge stations located in the wider area of the watershed basin. In addition, the land use and soil data were extracted after the application of object oriented nearest neighbor algorithms of ASTER satellite images. Subsequently, the CA-Markov chain analysis was implemented to predict the 2020 Land use/Land cover (LULC) map and incorporate it to the hydrological impact assessment. The results denoted the increase of runoff in the catchment area due to the recorded extensive urban sprawl phenomenon of the last decade.

1 Introduction

Landuse and floods are closely related; therefore, any changes in the land use, such as urbanization across the catchment's area, may trigger-off a sequence of flood occurrences (Hadjimitsis, 2010). The current and future development in water resources is very sensitive to land use and intensification of human activities. It is expected that flood risk will continue to rise, as a consequence of a combination of climate change (e.g. Kundzewicz et al., 2005; Tsanis et al., 2011; Grillakis et al., 2011) and an increase in exposurevulnerability (e.g., due to increasing flood plain occupancy), value increase in endangered areas and changes in the terrestrial system (e.g. land cover changes and river regulation; see Elmer et al., 2012). During the

GIS and RS techniques – land use changes impact on flood hydrology

D. D. Alexakis et al.

Title Page

Abstract

Introduction

Conclusions

References

Tables

Figures



Back

Close

Full Screen / Esc

Printer-friendly Version

Interactive Discussion



GIS and RS techniques – land use changes impact on flood hydrology

D. D. Alexakis et al.

Title Page

Abstract

Introduction

Conclusions

References

Tables

Figures

⏪

⏩

◀

▶

Back

Close

Full Screen / Esc

Printer-friendly Version

Interactive Discussion

past decades, airborne and spaceborne remote sensing technologies along with Geographical Information Systems (GIS) have become a key tool for flood monitoring, including flash floods (Taubenbock et al., 2011); Flash floods respond to the causative storms in a short period of time, with water levels in the drainage network reaching peak levels within a few minutes or hours, allowing for a very limited time-window for warnings to be prepared and issued (Koutroulis and Tsanis, 2010; Grillakis et al., 2010). Modeling of floods has greatly improved in recent years, with the advent of GIS, satellite remote sensing imagery, high-resolution digital elevation models (DEMs), distributed hydrologic models, and development of real time flood forecasting and delivery systems on the internet (Garrote and Bras, 1995; Bedient et al., 2003). Hydrological and hydraulic simulation models are essential tools to evaluate potential consequences of proposed strategies and to facilitate management decisions.

According to Mao and Cherkauer (2012), human activity is one of the major driving forces leading to changes in land cover characteristics and subsequently hydrologic processes. Land cover plays a key role in controlling the hydrologic regime of a catchment area through a number of different parameters such as leaf area index, evapotranspiration, soil moisture content and infiltration capacity, surface and subsurface flow regimes including base-flow contributions to streams and recharge, surface roughness, run off as well as soil erosion through complex interactions among vegetation, soils, geology, terrain and climate processes. According to Ragab and Cooper (1993), land use influences the infiltration and soil water distribution process because saturated hydraulic conductivity is influenced by plant roots and pores resulting from the presence of soil fauna. A characteristic example is the influence of build up areas and roads on overland flow, flood frequency and magnitude (Nejadhashemi et al., 2011).

Especially, urban areas are prone to flooding due to the large proportion of impermeable surface cover such as concrete that increases the total volume of runoff and peak flows and shortens the time that the floodwaters take to arrive at peak runoff (Hall, 1984; Knebl, 2005). In various studies, historical and present land-

GIS and RS techniques – land use changes impact on flood hydrology

D. D. Alexakis et al.

Title Page

Abstract

Introduction

Conclusions

References

Tables

Figures

⏪

⏩

◀

▶

Back

Close

Full Screen / Esc

Printer-friendly Version

Interactive Discussion



use/cover patterns or extreme scenarios have been used as input in hydrologic models to determine hydrologic responses to different scenarios in a combined integrated approach (Moiwo et al., 2010; Hong et al., 2010). At different watershed scales, several researchers (Savary et al., 2009; Schilling et al., 2010; Turnbull et al., 2012) have developed various methods aiming at quantifying the hydrologic alterations in relation to land-cover change. According to Xingan et al. (2012), the methods for detecting hydrologic responses to LULC are focused mainly on three aspects: (a) field-based experimentation for comparison, (b) statistical analysis based on observations, and (c) hydrologic modeling under different scenarios. Lin et al. (2007) refer to different models such as stochastic, optimization, dynamic process simulation and empirical ones, that have been used to explore the consequences of land use changes in hydrological modeling. In addition, researchers such as Chen et al. (2009) and Lin et al. (2007) have implemented sophisticated land use models (i.e., CLUE – Conversion of Land Use and its Effects) to simulate future land use changes. CLUE uses empirical quantified relationships between land use and its driving factors in combination with dynamic modeling.

This paper attempts to quantify the sensitivity of the distributed hydrological model to the land use and soil parameterizations, in order to simulate runoff processes in a catchment area in Cyprus, namely Yialias watershed. Specifically, the potential use of remote sensing in providing hydrological models with adequate, reliable and updated land use data is highlighted. The major flood event that occurred between 12–13 February 2003 was successively simulated with the use of multi-temporal land use data of the specific period (data of 2000) and data of 2010 (keeping the same meteorological parameters). The aim of this approach was to assess the impact of land use changes (including conversions between different land-use types and shifts in the geographic extent of those land-use types) to the run off processes and hydrologic response. In the following, a CA-Markov chain analysis was implemented to calculate and predict the area's LULC regime for 2020 and incorporate it to the hydrological model for assessing watershed's basin response.

2 Study area and data

Located in the central part of the island of Cyprus, the catchment area of the study is about 110 km² in size with an average slope value of 7.19% (Fig. 1). Specifically the study area is situated between longitudes 33°11'24, 28" and 33°26'31, 52" and latitudes 34°54'36, 74" and 35°2'52, 16" (WGS' 84, 36°N). In the past few years, the specific catchment area has been undergoing intensive land use change due to rapid economic growth and urbanization. The island of Cyprus is located in the northeastern-most corner of the Mediterranean Sea and, therefore, has a typical eastern Mediterranean climate: the combined temperature – rainfall regime is characterized by cool-to-mild wet winters and warm-to-hot dry summers (Michaelides et al., 2009).

For the purposes of the study, the following satellite and digital spatial data were utilized: (a) Two ASTER Images; the acquired ASTER images had a 10 yr time interval in order to monitor the multi-temporal urban sprawl phenomenon. For this study, the first three spectral bands were used (VNIR and SWIR) with spatial resolution of 15 m. The exact acquisition dates of the images were: 5 December 2000 and 4 June 2010. (b) A Digital Elevation Model (DEM) of 10 m pixel created with the use of ortho-rectified stereo-pairs of aerial photos (scale 1 : 5000) covering the study area.

The meteorological data were provided from the Meteorological Service of Cyprus. More specifically, a time-series rainfall dataset of 6 rain gauge stations for a period of 20 yr (1990–2010) was provided. Flow data from 3 stream gauges stations (Kotsiati, Nisou, Potamia) were provided from the Water Development Department of Cyprus (Table 1). The spatial distribution of rain and stream flow gauge stations in the vicinity of the catchment area shown in Fig. 2.

Title Page

Abstract

Introduction

Conclusions

References

Tables

Figures



Back

Close

Full Screen / Esc

Printer-friendly Version

Interactive Discussion

Atmospheric correction is considered to be one of the most difficult techniques since the distributions and intensities of these effects are often inadequately known. Despite the variety of techniques, used to estimate the atmospheric effect, atmospheric correction remains a hard task in the pre-processing of image data. As it is shown by several studies (Hadjimitsis et al., 2004, 2010; Agapiou et al., 2011), the darkest pixel (DP) atmospheric correction method can be easily and accurately applied either by using dark targets located in the image or by conducting in situ measurements. In the present study, water dams were used as dark targets and the darkest pixel correction was applied to both images.

3.2 Object oriented classification

According to Alexakis et al. (2012a), spectral mixing between marl/chalk geological formations and urban areas was widely observed in Yialias catchment area and especially in its downwards part. This problem is clearly denoted in the spectral signature diagram derived from the use of the handheld GER 1500 spectroradiometer. The GER 1500 spectroradiometer can record electromagnetic radiation between 350 nm up to 1050 nm. For the purposes of this study, five different targets from the Yialias watershed basin were selected and their corresponding samples were collected (Soil [Marl/Chalk] A, B, C, – Roof – Tile). Ten field measurements were consecutively carried out for each different sample. A final mean measurement corresponding to ASTER bands was extracted from the ten measurements and for this transformation the Relative Response Filters (RSR) of ASTER satellite was used. RSR filters describe the relative sensitivity of the satellite sensor to radiance at various parts of the electromagnetic spectrum (Wu et al., 2010) and their values range from 0 to 1. Bandpass filters are used in the same way in spectroradiometers in order to transmit a certain wavelength band and block others. Therefore, the broadband reflectance from the spectroradiometer was calculated based on the wavelength of ASTER sensor and

GIS and RS techniques – land use changes impact on flood hydrology

D. D. Alexakis et al.

Title Page

Abstract

Introduction

Conclusions

References

Tables

Figures

⏪

⏩

◀

▶

Back

Close

Full Screen / Esc

Printer-friendly Version

Interactive Discussion



GIS and RS techniques – land use changes impact on flood hydrology

D. D. Alexakis et al.

Title Page

Abstract

Introduction

Conclusions

References

Tables

Figures

◀

▶

◀

▶

Back

Close

Full Screen / Esc

Printer-friendly Version

Interactive Discussion



compared to object's shape, was set to 0.1 in order to give less weight to shape since urban and marl/chalk classes did not have a specific shape. The compactness parameter balances compactness/smoothness and determines the object shape between compact edges and smooth boundaries. It was set to 0.5 in order to balance equally the compactness and smoothness of the objects. However, the most crucial factor of segmentation process is the adjustment of scale which controls the object size. Thus, the higher the value of scale parameter, the larger the extracted segmented objects. Following, the evaluation of several different scale parameters, a value of 10 was selected. Thus, the images were initially segmented (Fig. 4c) into object primitives or segments using the multi-resolution algorithm which according to Baatz et al. (2003) follows the fractal net evolution algorithm.

The classification process identified and implemented seven major different classes (Agriculture Generic, Agriculture Close Green, Herbaceous, Forest Mixed, Olive Trees, Urban fabric, Water) by using the nearest neighbour classification algorithm (Fig. 5b, c). The main advantage of the nearest neighbour classification algorithm is that it allows unlimited applicability of the classification process to other areas and requires only the additional selection of new training samples until a satisfactory result is obtained.

At the end, with the specific classification approach, the Kappa coefficient values were increased from the initial values of lower to 0.6 to 0.78 and 0.80 for 2000 and 2010 cases, accordingly.

3.3 Soil map

The soil map was constructed in GIS environment according to local hydrogeological maps regime, local soil data and HEC-HMS soil classes. The final map was a three classes generalised soil map of the area (Fig. 6).

4 Prediction of urban sprawl phenomenon

The Stochastic Markov chain Model was implemented to test whether urban expansion could be predicted for 2020 using the ASTER data of both 2000 and 2010. According to Ahmed and Ahmed (2012), this kind of predictive land cover change modeling is appropriate when the past trend of land cover is known.

Urban growth modeling has evolved over recent years to capture increasingly well the details of urban morphology and structure at a qualitative as well as a quantitative level (Rimal, 2005). Land use change transition probability in Markov analysis indicates the probability of making a transition from one land use class to another within two discrete time periods. The Markov chain equation was constructed using the land cover distributions at the beginning (M_t) and at the end (M_{t+1}) of a discrete time period, as well as a transition matrix (MLC) representing the land cover changes that occurred during that period. In a Markov chain the probability of the next state is only dependent upon the current state. This is called Markov property as shown in the Eq. (2) (Ahmed and Ahmed, 2012):

$$P(\xi_{t+1} = X_{i_{t+1}} | \xi_1 = X_{i_1}, \dots, \xi_t = X_{i_t}) = P(\xi_{t+1} = X_{i_{t+1}} | \xi_t = X_{i_t}) \quad (2)$$

where, the probability Markov chain ξ_1, ξ_2, \dots can be calculated as:

$$P(\xi_1 = X_{i_1}, \dots, \xi_t = X_{i_t}) = P(\xi_1 = X_{i_1}) \cdot P(\xi_2 = X_{i_2} | \xi_1 = X_{i_1}) \cdot P(\xi_t = X_{i_t}) \cdot P(\xi_{t-1} = X_{i_{t-1}}) \quad (3)$$

Under the assumption that the sample is representative of the region, these proportional changes become probabilities of land cover change over the entire sample area and form the transition matrices. However, the model is not spatially explicit and does not provide explanation the processes leading to changes and overlooks the spatial distribution of land cover in predicting land cover (Lambin et al., 1994; Adhikari et al., 2012).

Title Page

Abstract

Introduction

Conclusions

References

Tables

Figures

⏪

⏩

◀

▶

Back

Close

Full Screen / Esc

Printer-friendly Version

Interactive Discussion



GIS and RS techniques – land use changes impact on flood hydrology

D. D. Alexakis et al.

Title Page

Abstract

Introduction

Conclusions

References

Tables

Figures

⏪

⏩

◀

▶

Back

Close

Full Screen / Esc

Printer-friendly Version

Interactive Discussion

The transition probability matrix explains the probability that each land cover category will change into another category. Specifically, it refers to the number of pixels that are expected to change from each land cover type to every other type over the specified number of time units (Kityuttachai et al., 2013). A combined Markov and CA (CA-Markov) was used to predict the area's land cover regime for the year 2020. The CA-Markov analysis was run to test a pair of land cover images (2000 and 2010) and output the transition probability matrix (Table 2). As it is indicated in Table 2, the Forest Mixed and Olive Trees classes have significant possibility to change to urban land cover in the near future.

After the implementation of CA-Markov model, the land use area statistics were thoroughly examined (Fig. 7a). The results indicated a steady increase of land cover within the catchment area which is expected to range in a percentage of around 100% until 2020. Part of this expansion is indicated in Fig. 7b. In addition, significant decrease of agricultural close grown land cover is recorded for 2010 and is predicted for 2020.

5 Hydrological modeling

5.1 The hydrological model HEC-HMS

The Hydrologic Modeling System (HEC-HMS) is designed to simulate the precipitation-runoff processes of dendritic watershed systems. It is designed to be applicable in a wide range of geographic areas for solving the widest possible range of problems. This includes large river basin water supply and flood hydrology and small urban or natural watershed runoff (HEC-HMS User's Manual, 2001).

The basic rainfall runoff processes that need to be simulated in HEC-HMS for flood flow estimation using rainfall data as input are the rainfall losses and the transformation of excess rainfall to runoff. For calculating rainfall losses the SCS Curve Number method was used and for the transformation of excess rainfall to runoff the ModClark method was used.

5.2 The ModClark method

The modified Clark (ModClark) model in HEC-HMS is a distributed parameter model in which spatial variability of characteristics and processes are considered explicitly (Kull and Feldman, 1998; Peters and Easton, 1996). This model accounts explicitly for variations in travel time to the watershed outlet from all regions of a watershed. The ModClark algorithm is a version of the Clark unit hydrograph transformation modified to accommodate spatially distributed precipitation (Clark, 1945). Runoff computations with the ModClark model explicitly account for translation and storage. Storage is accounted for within the same linear reservoir model incorporated in the Clark model. Translation is accounted for within a grid-based travel-time model $t_{\text{cell}} = t_c \cdot (d_{\text{cell}}/d_{\text{max}})$ (HEC, 2000), where t_c is the time of concentration for the subwatershed and is a function of basin's length and slope, d_{cell} is the travel distance from the cell to the outlet, and d_{max} is the travel distance from the cell furthest from the outlet. The method requires an input coefficient for storage, R , where R accounts for both translation and attenuation of excess precipitation as it moves over the basin toward the outlet. Storage coefficient R is estimated as the discharge at the inflection point on the recession limb of the hydrograph divided by the slope at the inflection point. The translation hydrograph is routed using the equation:

$$Q(t) = \left[\frac{\Delta t}{R + 0.5\Delta t} I(t) \right] + \left[1 - \frac{\Delta t}{R + 0.5\Delta t} Q(t-1) \right] \quad (4)$$

where, $Q(t)$ is the outflow from storage at time t , Δt is the time increment, R is the storage coefficient, $I(t)$ is the average inflow to storage at time t and $Q(t-1)$ is the outflow from storage at previous time $(t-1)$.

5.3 SCS curve number loss method

The SCS (Soil Conservation Service) curve number loss method is a simple, widely used and efficient method for computing excess rainfall (direct runoff) from a rainfall

Title Page

Abstract

Introduction

Conclusions

References

Tables

Figures

⏪

⏩

◀

▶

Back

Close

Full Screen / Esc

Printer-friendly Version

Interactive Discussion



event in a particular area. The curve number is based on the area's hydrologic soil group, land use, treatment and hydrologic condition, with the first two having the greatest importance. The SCS runoff curve number (CN) method is described in detail in NEH (National Engineering Handbook) – 4 (SCS, 1985). The SCS runoff equation is:

$$Q = \frac{(P - IA)^2}{(P - IA) + S} \quad (5)$$

where Q is the runoff volume, P the precipitation volume, IA is the initial abstraction and S field capacity.

A linear relationship between IA and S was suggested by SCS (1985), as shown in Eq. (6).

$$IA = \lambda \times S \quad (6)$$

where, λ = initial abstraction ratio. With $\lambda = 0.2$ in Eq. (3), Eq. (2) is transformed into the following equation:

$$Q = \frac{(P - 0,2S)^2}{P + 0,8S} \quad (7)$$

For convenience in practical applications, S is mapped into a dimensionless parameter CN (i.e., the curve number) which varies in the more appealing range between 0 and 100. The chosen mapping equation is presented as follows, for SI units.

$$S = \frac{25\,400 - 254CN}{CN} \quad (8)$$

5.4 Performance estimators

5.4.1 Nash–Sutcliffe efficiency E

The efficiency E proposed by Nash and Sutcliffe (1970) is defined as one minus the sum of the absolute squared differences between the predicted and observed

GIS and RS techniques – land use changes impact on flood hydrology

D. D. Alexakis et al.

Title Page

Abstract

Introduction

Conclusions

References

Tables

Figures

⏪

⏩

◀

▶

Back

Close

Full Screen / Esc

Printer-friendly Version

Interactive Discussion



values normalized by the variance of the observed values during the period under investigation. It is estimated by equation:

$$E = 1 - \frac{\sum_{i=1}^n (O_i - P_i)^2}{\sum_{i=1}^n (O_i - \bar{O})^2} \quad (9)$$

where, O indicates observed and P predicted values; bars indicate mean values. The normalization of the variance of the observation series results in relatively higher values of E in catchments with higher dynamics and lower values of E in catchments with lower dynamics. To obtain comparable values of E in a catchment with lower dynamics, the prediction has to be better than in a basin with high dynamics. The range of E lies between 1.0 (perfect fit) and $-\infty$. A result lower than zero indicates that the mean value of the observed time series would have been a better predictor than the model.

5.4.2 Phase error (PE)

Phase error is defined as the difference in hours between the peak of the observed and the simulated flow.

5.4.3 Peak discharge error (PD_{err})

Peak discharge error is defined as the percent difference between the observed and the simulated peak discharges:

$$PD_{err} = \frac{\max Q_{sim} - \max Q_{obs}}{\max Q_{obs}} \times 100 \quad (10)$$

GIS and RS techniques – land use changes impact on flood hydrology

D. D. Alexakis et al.

Title Page

Abstract

Introduction

Conclusions

References

Tables

Figures

⏪

⏩

◀

▶

Back

Close

Full Screen / Esc

Printer-friendly Version

Interactive Discussion



6 Case study

6.1 Model set up

The HEC-HMS model was setup in distributed mode, enabling the utilization of the spatial information of the land use via the Curve Number coefficient. The rainfall losses component was based solely on the SCS curve number method (USDA SCS, 1972). This method assumes an initial abstraction before ponding that is related to curve number. Curve numbers in this study were determined from USDA National Engineering Handbook (USDA-SCS, 1972). The curve number method in HEC-HMS relates runoff to soil type, land use management and antecedent soil moisture conditions. The transformation method used was the modified Clark that considers the spatial variability of characteristics and processes explicitly. The Curve number was estimated using a 10 m resolution digital elevation model, land use classification for 2000 and soil classification of the area.

Three sub basins were considered in the basin model, according to the three available flow gauging station. The HEC-HMS model was calibrated using three available rainfall – runoff events (2000, 2001, 2004), while was validated in a flood event. A list of the rainfall runoff events is given in Table 1.

The specific event occurred in the watershed's urban area (downwards) between 12–13 (peak time) February 2003. During this event, a driver of a school bus was deadly injured and severe damages were caused all over the catchment area. A list of the rainfall runoff events is given in Table 3.

7 Results

The calibration of the model was performed using the Nash–Sutcliffe estimator (E), with respect to the correct representation of the peak discharge and the correct timing of it. The calibration and validation results are shown in Table 3.

NHESSD

1, 4833–4869, 2013

GIS and RS techniques – land use changes impact on flood hydrology

D. D. Alexakis et al.

Title Page

Abstract

Introduction

Conclusions

References

Tables

Figures

⏪

⏩

◀

▶

Back

Close

Full Screen / Esc

Printer-friendly Version

Interactive Discussion



GIS and RS techniques – land use changes impact on flood hydrology

D. D. Alexakis et al.

Title Page

Abstract

Introduction

Conclusions

References

Tables

Figures



Back

Close

Full Screen / Esc

Printer-friendly Version

Interactive Discussion

The calibration and validation hydrographs are presented in Fig. 8. The results of the calibration show that the distributed setup of HEC-HMS model adequately describes the hydrology of Yialias basin. E ranged from 0.9 to 0.46 between the calibration events and the three sub basins. For the validation event, the E ranged between 0.45 and 0.62. The phase error ranged between 0 and 1 h, except for Event 2 and 3 (Table 3) simulation at Potamia that the phase error was two hours. Finally, the peak discharge error was kept under 17.6%, in all sub basins and calibration events, while for the validation event, it ranged between 0% and 6%.

Having calibrated and validated the HEC-HMS model, the land use map of 2010 and the projected 2020 were used to estimate the changed curve number map for 2010 and 2020, respectively (Fig. 9).

The changes between the 2000 curve number and the ones of 2010 and 2020 are also demonstrated in Fig. 10. All the events that were used to calibrate and validate the hydrological model were then run under changed land use conditions. The results are shown in Table 4.

The results show an increase in the peak discharge. The magnitude of the increase in peak flow was different for the four simulated events and for each subbasin in the catchment.

Results for the validation event (which consisted a flood event in 2003), indicate an increase in the runoff response under the changed land use conditions of 2010. The changes were estimated to be 10.2%, 7% and 11.1% (Table 4), for the three sub-basins Kotsiatis, Nisou and Potamia, respectively, in comparison to those of 2000. The outcome indicates that the runoff dynamics of the basin are changing due to the landuse transition among different categories. Next, the CA-Markov chain predicted 2020 land use was used to simulate the 2003 event under future land use conditions. The results show a noteworthy increase in the peak discharge that reached 22.4% 14.6% and 19.9% compared to the 2000 land use runs for the above three subbasins, respectively. The simulated changes in the runoff are presented in Fig. 11.

8 Conclusions

This study presented an integrated methodology for searching and forecasting a catchment area's hydrologic response with the use of HEC-HMS model and satellite remote sensing techniques. The preliminary results denoted the crucial role of urban sprawl phenomenon in the increase of runoff rate within the spatial limits of a catchment area and highlighted the importance of searching land use regime with the use of satellite remote sensing imageries. It was proved that the incorporation of multitemporal remote sensing data in hydrological models can effectively support decision making in the areas of risk and vulnerability assesment, sustainable development and general managment before and after flood events. In addition, the implementation of CA-Marcov model gave the opportunity to predict the catchment area's flood vulnerability in the near future.

The comparison of observed flow results concerning the flood event of 2003 with the simulated flow results (with the use of different land use data concerning 2000, 2010 and 2020 land use regime) proved that in the case of "2010" and "2020" model, the runoff rates were steadily higher due to the expanded urban area cover that increased the phenomenon of surface run off. This tendency was verified after incorportating the land use data for the 2020 time period. Knowing from past events that the area between the Nisou and Potamia is highly prone to flooding, the already increased dynamics of the surface runoff indicate higher flooding hazard for the area. Moreover, the projected changes in land use that is simulated to increase the peak discharge by 14.6 % and 19.9 % until 2020 for the Nisou and Potamia, dictate actions have to be taken to mitigate the flood hazard.

The results of this study can be used as a road map for taking specific actions in land use management changes to achive sustainable water resources goals in the near future. The research team will continue to study the hydrological response of the catchment area with more updated meteorological and stream data as well as satellite images of higher spatial resolution.

GIS and RS techniques – land use changes impact on flood hydrology

D. D. Alexakis et al.

Title Page

Abstract

Introduction

Conclusions

References

Tables

Figures



Back

Close

Full Screen / Esc

Printer-friendly Version

Interactive Discussion



Acknowledgements. The project is funded by the Cyprus Research Promotion Foundation in the frameworks of the project “SATFLOOD” (ΠΡΟΣΕΛΚΥΣΗ/ΝΕΟΣ/0609). Also, thanks are given to the Remote Sensing and Geo Environment Laboratory of the Department of Civil Engineering and Geomatics at the Cyprus University of Technology for supporting this project (http://www.cyprusremotesensing.com/).

References

- Adhikari, S. and Southworth, J.: Simulating forest cover changes of Bannerghatta National Park based on a CA-Markov model: a remote sensing approach, *Remote Sensing*, 4, 3215–3243, 2012.
- Agapiou, A., Hadjimitsis, D. G., Papoutsas, C., Alexakis, D. D., and Papadavid, G.: The importance of accounting for atmospheric effects in the application of NDVI and interpretation of satellite imagery supporting archaeological research: the case studies of Palaepaphos and Nea Paphos sites in Cyprus, *Remote Sensing*, 3, 2605–2629, doi:10.3390/rs3122605, 2011.
- Ahmed, B. and Ahmed, R.: Modelling urban land cover growth dynamics using multi-temporal satellite images: a case study of Dhaka, Bangladesh, *ISPRS Int. J. Geo-Inf.*, 1, 3–31, 2012.
- Alexakis, D., Agapiou, A., Hadjimitsis, D. G., and Retalis, A.: Optimizing statistical classification accuracy of satellite remotely sensed imagery for supporting fast flood hydrological analysis, *Acta Geophys.*, 60, 959–984, 2012a.
- Alexakis, D. D., Hadjimitsis, D. G., Agapiou, A., Themistocleous, K., and Retalis, A.: Monitoring urban land cover using satellite remote sensing techniques and field spectroradiometric measurements: the case study of Yialias catchment area in Cyprus, *J. Appl. Remote Sens.*, 6, 063603, doi:10.1117/1.JRS.6.063603, 2012b.
- Batz, M. and Schape, A.: Multiresolution segmentation – an optimization approach for high quality multi-scale image segmentation, in: *Angewandte Geographische Informationsverarbeitung XII*, edited by: Strobl, J., Blaschke, T., and Griesebner, G., Wichmann-Verlag, Heidelberg, 12–23, 2000.
- Batz, M., Benz, U., Dehghani, S., Heynen, M., Holtje, A., Hofmann, P., Lingenfelder, I., Mimler, M., Sohlbach, M., Weber, M., and Willhauck, G.: *eCognition Professional: User Guide 4*, Definiens-Imaging, Munich, 2004.

GIS and RS techniques – land use changes impact on flood hydrology

D. D. Alexakis et al.

Title Page

Abstract

Introduction

Conclusions

References

Tables

Figures

⏪

⏩

◀

▶

Back

Close

Full Screen / Esc

Printer-friendly Version

Interactive Discussion



GIS and RS techniques – land use changes impact on flood hydrology

D. D. Alexakis et al.

Title Page

Abstract

Introduction

Conclusions

References

Tables

Figures

⏪

⏩

◀

▶

Back

Close

Full Screen / Esc

Printer-friendly Version

Interactive Discussion



- Bedient, P. B., Holder, A., Benavides, J. A., and Vieux, B. E.: Radar-based flood warning system applied to tropical storm Allison, *J. Hydrol. Eng.*, 8, 308–318, 2003.
- Boegh, E., Poulsen, R. N., Butts, M., Abrahamsen, P., Dellwik, E., Hansen, S., Hasager, C. B., Ibrom, A., Loerup, J. K., Pilegaard, K., and Soegaard, H.: Remote sensing based evapotranspiration and runoff modeling of agricultural, forest and urban flux sites in Denmark: from field to macro-scale, *J. Hydrol.*, 377, 300–316, 2009.
- Chen, Y., Xu, Y., and Yin, Y.: Impacts of land use change scenarios on storm-runoff generation in Xitiaoxi Basin, China, *Quatern. Int.*, 208, 121–128, 2009.
- Clark, C. O.: Storage and the unit hydrograph, *T. Am. Soc. Civ. Eng.*, 110, 1419–1488, 1945.
- Definiens AG: Definiens Developer 7.0, User Guide, Munich, Germany, 506 pp., 2008.
- Elmer, F., Hoymann, J., Dühmann, D., Vorogushyn, S., and Kreibich, H.: Drivers of flood risk change in residential areas, *Nat. Hazards Earth Syst. Sci.*, 12, 1641–1657, doi:10.5194/nhess-12-1641-2012, 2012.
- Garrote, L. and Bras, R. L.: A distributed model for real-time flood forecasting using digital elevation models, *J. Hydrol.*, 16, 279–306, 1995.
- Giertz, S., Diekkrüger, B., Jaeger, A., and Schopp, M.: An interdisciplinary scenario analysis to assess the water availability and water consumption in the Upper Ouémé catchment in Benin, *Adv. Geosci.*, 9, 3–13, doi:10.5194/adgeo-9-3-2006, 2006.
- Grillakis, M. G., Tsanis, I. K., and Koutroulis, A. G.: Application of the HBV hydrological model in a flash flood case in Slovenia, *Nat. Hazards Earth Syst. Sci.*, 10, 2713–2725, doi:10.5194/nhess-10-2713-2010, 2010.
- Grillakis, M. G., Koutroulis, A. G., and Tsanis, I. K.: Climate change impact on the hydrology of Spencer Creek watershed in southern Ontario, Canada, *J. Hydrol.*, 409, 1–19, 2011.
- Hadjimitsis, D. G.: Brief communication “Determination of urban growth in catchment areas in Cyprus using multi-temporal remotely sensed data: risk assessment study”, *Nat. Hazards Earth Syst. Sci.*, 10, 2235–2240, doi:10.5194/nhess-10-2235-2010, 2010.
- Hadjimitsis, D. G., Clayton, C. R. I., and Hope, V. S.: An assessment of the effectiveness of atmospheric correction algorithms through the remote sensing of some reservoirs, *Int. J. Remote Sens.*, 25, 3651–3674, 2004.
- Hall, M. J.: *Urban Hydrology*, Elsevier Applied Science Publishers, Northern Ireland, 1984.
- HEC: *Hydrologic Modeling System: Technical Reference Manual*, US Army Corps of Engineers Hydrologic Engineering Center, Davis, CA, 2000.

**GIS and RS
techniques – land
use changes impact
on flood hydrology**

D. D. Alexakis et al.

Title Page

Abstract

Introduction

Conclusions

References

Tables

Figures

⏪

⏩

◀

▶

Back

Close

Full Screen / Esc

Printer-friendly Version

Interactive Discussion



Peters, J. C. and Easton, D. J.: Runoff simulation using radar rainfall data, *J. Am. Water Resour. As.*, 32, 753–760, doi:10.1111/j.1752-1688.1996.tb03472.x, 1996.

Ragab, R. and Cooper, J. D.: Variability of unsaturated zone water transport parameters: implications for hydrological modelling. 1. In situ measurements, *J. Hydrol.*, 148, 109–131, 1993.

Savary, S., Rousseau, A. N., and Quilbé, R.: Assessing the effects of historical land cover changes on runoff and low flows using remote sensing and hydrological modeling, *J. Hydrol. Eng.*, 14, 575–587, 2009.

Schilling, K. E., Chan, K. S., Liu, H., and Zhang, Y. K.: Quantifying the effect of land use land cover change on increasing discharge in the Upper Mississippi River, *J. Hydrol.*, 387, 343–345, 2010.

SCS: National Engineering Handbook, “Section 4: Hydrology.” Soil Conservation Service, USDA, Washington, DC, 1985.

Stephens, E. M., Bates, P. D., Freer, J. E., and Mason, D. C.: The impact of uncertainty in satellite data on the assessment of flood inundation models, *J. Hydrol.*, 414–415, 162–173, 2012.

Stow, D., Lopez, A., Lippitt, C., Hinton, S., and Weeks, J.: Object-based classification of residential land use within Accra, Ghana based on QuickBird satellite data, *Int. J. Remote Sens.*, 28, 5167–5173, 2007.

Taubenböck, H., Wurm, M., Netzband, M., Zwenzner, H., Roth, A., Rahman, A., and Dech, S.: Flood risks in urbanized areas – multi-sensoral approaches using remotely sensed data for risk assessment, *Nat. Hazards Earth Syst. Sci.*, 11, 431–444, doi:10.5194/nhess-11-431-2011, 2011.

Te Linde, A. H., Bubeck, P., Dekkers, J. E. C., de Moel, H., and Aerts, J. C. J. H.: Future flood risk estimates along the river Rhine, *Nat. Hazards Earth Syst. Sci.*, 11, 459–473, doi:10.5194/nhess-11-459-2011, 2011.

Tsanis, I. K., Koutroulis, A. G., Daliakopoulos, I. N., and Jacob, D.: Severe climate induced water shortage and extremes in Crete, *Climatic Change*, 106, 667–677, 2011.

Turnbull, L., Wainwright, J., and Brazier, R. E.: Changes in hydrology and erosion over a transition from grassland to shrubland, *Hydrol. Process.*, 24, 393–414, 2010.

US Department of Agriculture, Soil Conservation Service: National Engineering Handbook, Hydrology Sect. 4, Chapt. 4–10, USDA, Washington, DC, 1972.

NHESSD

1, 4833–4869, 2013

GIS and RS techniques – land use changes impact on flood hydrology

D. D. Alexakis et al.

Title Page

Abstract Introduction

Conclusions References

Tables Figures

⏪ ⏩

◀ ▶

Back Close

Full Screen / Esc

Printer-friendly Version

Interactive Discussion

Whiteside, T., Boggs, G., and Maier, S.: Comparing object-based and pixel-based classifications for mapping savannas, *Int. J. Appl. Earth Obs.*, 13, 884–893, 2011.

Willhauck, G., Schneider, T., De Kok, R., and Ammer, U.: Comparison of object oriented classification techniques and standard image analysis for the use of change detection between SPOT multispectral satellite images and aerial photos, in: *Proceedings of XIX ISPRS Congress, Amsterdam, 16–22 July 2000, 2000.*

5 Wu, X., Sullivan, T. J., and Heidinger, K. A.: Operational calibration of the advanced very high resolution radiometer (AVHRR) visible and near-infrared channels, *Can. J. Remote Sens.*, 36, 602–616, 2010.

10 Zhang, X., Liu, Y., Fang, Y., Liu, B., and Xia, D.: Modeling and assessing hydrologic processes for historical and potential land-cover change in the Duoyingping watershed, southwest China, *Phys. Chem. Earth*, 53–54, 19–29, 2012.



GIS and RS techniques – land use changes impact on flood hydrology

D. D. Alexakis et al.

Title Page

Abstract

Introduction

Conclusions

References

Tables

Figures

◀

▶

◀

▶

Back

Close

Full Screen / Esc

Printer-friendly Version

Interactive Discussion

Table 1. Characteristics of the study area's rain and flow gauge stations.

Stations	Longitude Easting	Latitude Northing	Elevation (m)	Distance from the coast (km)	Length of records (year)
<i>Rain gauges</i>					
1 Mantra tou Kampiou	52°06'82"	38°67'871"	640	21.818	20
2 Analiontas	52°65'62"	38°74'143"	360	27.124	20
3 Lithrodontas	52°74'20"	38°67'428"	420	20.926	20
4 Leukara	52°67'83"	38°61'720"	420	16.28	20
5 Kionia	51°82'69"	38°63'820"	1200	13.97	20
6 Pera Chorio	53°54'07"	38°74'471"	250.38	24.02	20
7 Mathiatis	53°06'15"	38°69'030"	373.78	25.23	20
<i>Flow gauges</i>					
1 Kotsiati	53°97'79"	38°78'282"	195.43	27.75	34
2 Nisou	53°59'60"	38°75'415"	239.99	24.45	46
3 Potamia	53°06'39"	38°72'576"	298.91	22.05	14

GIS and RS techniques – land use changes impact on flood hydrology

D. D. Alexakis et al.

Table 2. Transition probability matrix for each land covers class using the Markov chain equation.

	Agricultural – Close Grown	Agricultural – Generic	Herbaceous	Forest Mixed	Urban	Olive Trees	Water
1 Agricultural – Close Grown	0.8157	0.0340	0.0500	0.0237	0.0158	0.0606	0.00
2 Agricultural – Generic	0.0004	0.8070	0.1551	0.0007	0.0001	0.0367	0
3 Herbaceous	0.0721	0.0986	0.6058	0.0767	0.0296	0.1171	0.0001
4 Forest Mixed	0.2963	0.1509	0.1329	0.3222	0.0568	0.0409	0
5 Urban	0.1925	0.0995	0.1747	0.0485	0.3433	0.1398	0.0017
6 Olive Trees	0.0983	0.1370	0.2084	0.1556	0.0549	0.3458	0
7 Water	0	0	0.4222	0	0.0889	0.0667	0.4222

Title Page

Abstract

Introduction

Conclusions

References

Tables

Figures

⏪

⏩

◀

▶

Back

Close

Full Screen / Esc

Printer-friendly Version

Interactive Discussion

GIS and RS techniques – land use changes impact on flood hydrology

D. D. Alexakis et al.

Table 3. Calibration and validation results of HEC-HMS. The Nash–Sutcliffe (E), Phase Error (PE) and Peak Discharge Error (PDE) are presented. Negative values of phase error (PE) indicate simulated peak before the observed event.

		Kotsiatis			Nisou			Potamia		
		E	PE [h]	PDE [%]	E	PE [h]	PDE [%]	E	PE [h]	PDE [%]
Calibration	Event 1	0.78	0	3.3	0.87	1	−0.6	0.46	1	5.6
	Event 2	0.61	0	0.0	0.66	1	4.7	0.86	2	4.6
	Event 3	0.67	0	−1.2	0.70	1	17.6	0.90	2	4.8
Validation	Event 4	0.45	0	0.0	0.50	1	2.5	0.62	0	6.0

[Title Page](#)
[Abstract](#)
[Introduction](#)
[Conclusions](#)
[References](#)
[Tables](#)
[Figures](#)
[Back](#)
[Close](#)
[Full Screen / Esc](#)
[Printer-friendly Version](#)
[Interactive Discussion](#)

GIS and RS techniques – land use changes impact on flood hydrology

D. D. Alexakis et al.

Table 4. Changes in Yialias simulated peak discharge due to land cover change in 2010 and 2020 comparing to the 2000 land use.

	Kotsiatis		Nisou		Potamia	
	2010	2020	2010	2020	2010	2020
Event 1	39.4 %	59.4 %	32.1 %	49.1 %	56.6 %	88.2 %
Event 2	1.9 %	4.5 %	1.5 %	3.7 %	1.5 %	4.4 %
Event 3	11.1 %	20.2 %	7.1 %	12.3 %	7.7 %	12.7 %
Event 4	10.2 %	22.4 %	7.0 %	14.6 %	11.1 %	19.9 %

Title Page

Abstract

Introduction

Conclusions

References

Tables

Figures

⏪

⏩

◀

▶

Back

Close

Full Screen / Esc

Printer-friendly Version

Interactive Discussion

GIS and RS techniques – land use changes impact on flood hydrology

D. D. Alexakis et al.

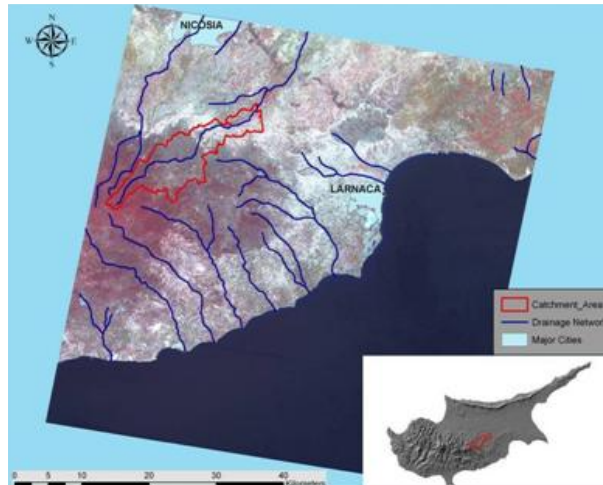


Fig. 1. Study area as indicated in the RGB- 321 of ASTER image.

Title Page

Abstract

Introduction

Conclusions

References

Tables

Figures



Back

Close

Full Screen / Esc

Printer-friendly Version

Interactive Discussion



GIS and RS techniques – land use changes impact on flood hydrology

D. D. Alexakis et al.

Title Page

Abstract

Introduction

Conclusions

References

Tables

Figures



Back

Close

Full Screen / Esc

Printer-friendly Version

Interactive Discussion

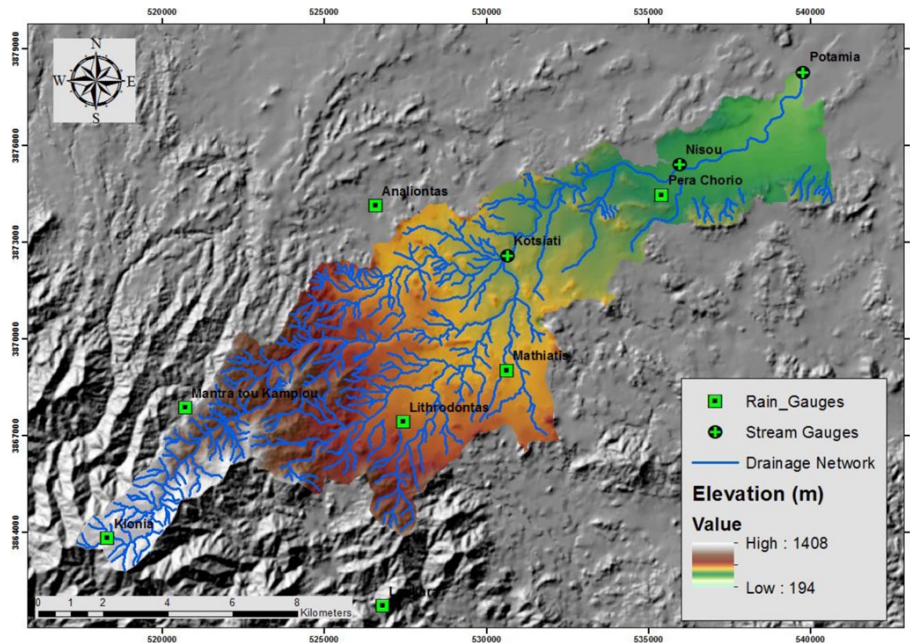


Fig. 2. Location of rain and stream gauges stations.

GIS and RS techniques – land use changes impact on flood hydrology

D. D. Alexakis et al.

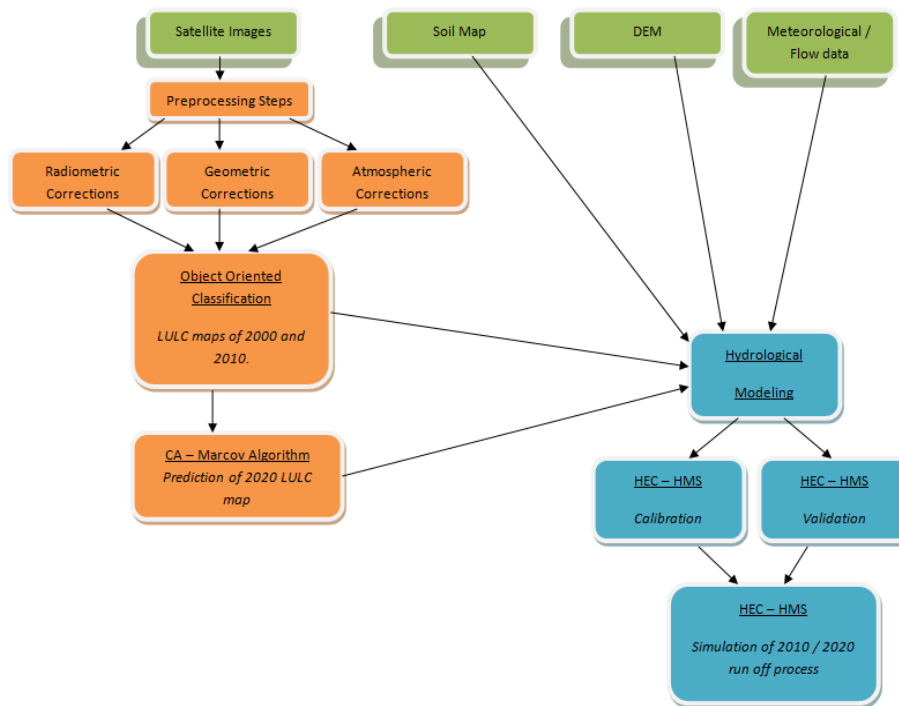


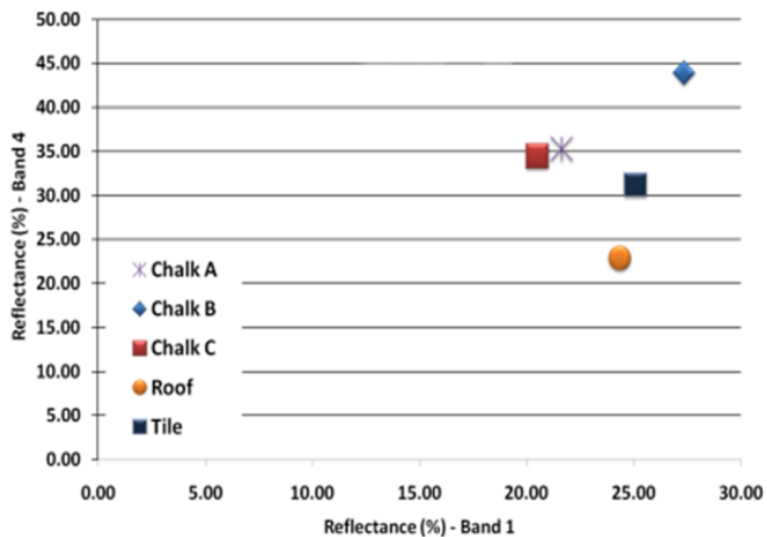
Fig. 3. Flow chart of the proposed methodology.

Title Page	
Abstract	Introduction
Conclusions	References
Tables	Figures
◀	▶
◀	▶
Back	Close
Full Screen / Esc	
Printer-friendly Version	
Interactive Discussion	



**GIS and RS
techniques – land
use changes impact
on flood hydrology**

D. D. Alexakis et al.

**Fig. 4.** Scatter plot for the different targets for bands 1–4.[Title Page](#)[Abstract](#)[Introduction](#)[Conclusions](#)[References](#)[Tables](#)[Figures](#)[◀](#)[▶](#)[◀](#)[▶](#)[Back](#)[Close](#)[Full Screen / Esc](#)[Printer-friendly Version](#)[Interactive Discussion](#)

GIS and RS techniques – land use changes impact on flood hydrology

D. D. Alexakis et al.

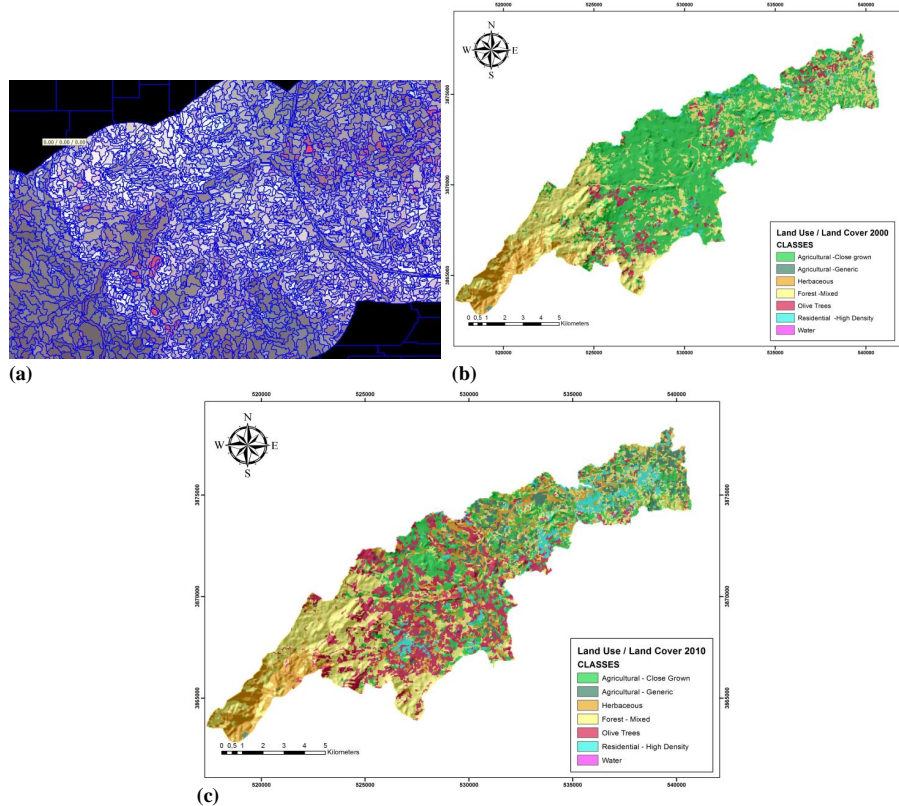


Fig. 5. (a) Image segmentation of ASTER 2010 image; (b) LULC map of the study area for 2000; and (c) LULC map of the study area for 2010.

Title Page

Abstract

Introduction

Conclusions

References

Tables

Figures

⏪

⏩

◀

▶

Back

Close

Full Screen / Esc

Printer-friendly Version

Interactive Discussion



GIS and RS techniques – land use changes impact on flood hydrology

D. D. Alexakis et al.

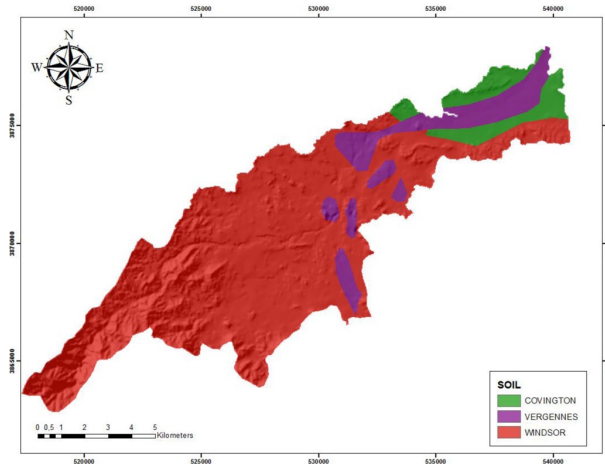


Fig. 6. Soil map of the study area.

Title Page	
Abstract	Introduction
Conclusions	References
Tables	Figures
◀	▶
◀	▶
Back	Close
Full Screen / Esc	
Printer-friendly Version	
Interactive Discussion	

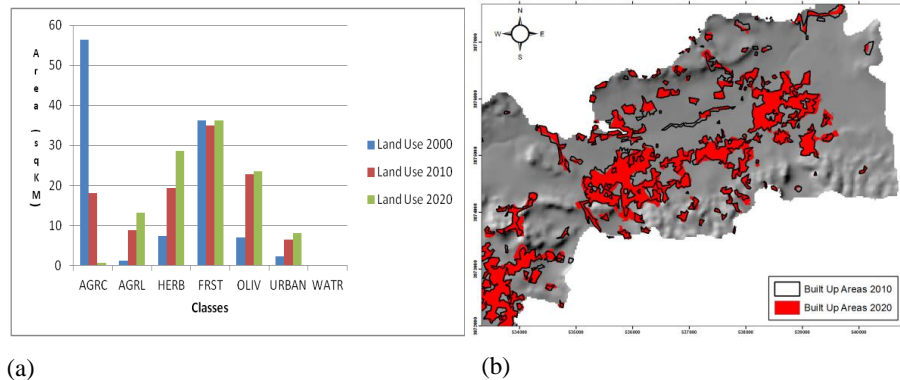


Fig. 7. (a) Land use statistics (AGRC = Agricultural Close Grown, AGRL = Agricultural, HERB = Herbaceous, FRST = Forest Mixed, OLIV = Olive Trees, URBAN = Urban Fabric, WATR = Water). **(b)** Detail of the downwards of the catchment area indicating urban regime for the next decade.

Title Page

Abstract

Introduction

Conclusions

References

Tables

Figures

◀

▶

◀

▶

Back

Close

Full Screen / Esc

Printer-friendly Version

Interactive Discussion

GIS and RS techniques – land use changes impact on flood hydrology

D. D. Alexakis et al.

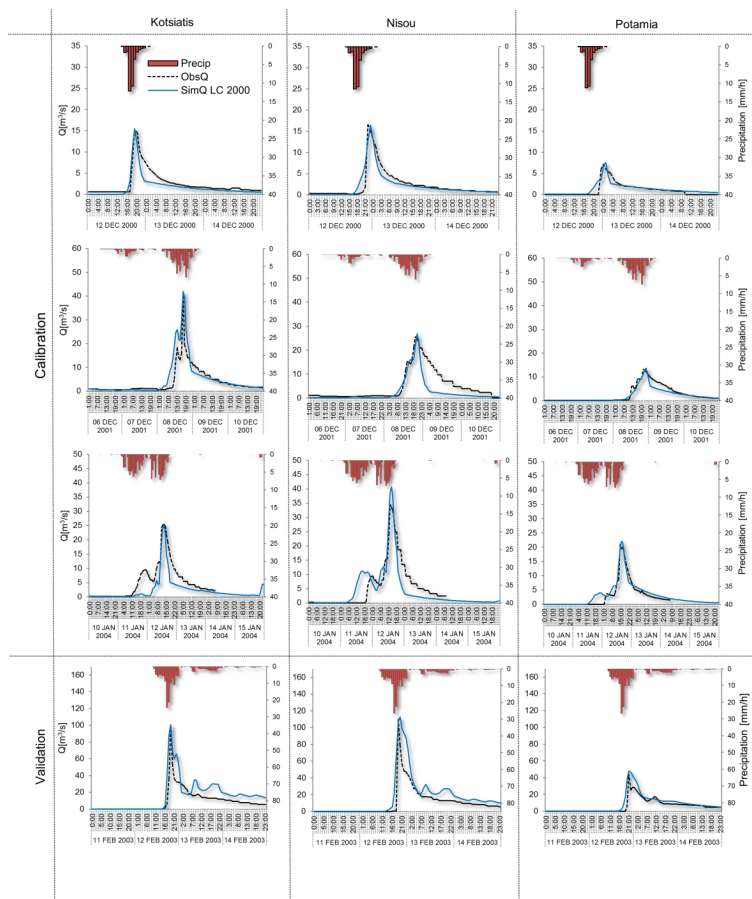


Fig. 8. Calibration and validation hydrographs for the observed and simulated flows.

Title Page

Abstract	Introduction
Conclusions	References
Tables	Figures

⏪	⏩
◀	▶
Back	Close

Full Screen / Esc

Printer-friendly Version

Interactive Discussion



GIS and RS techniques – land use changes impact on flood hydrology

D. D. Alexakis et al.

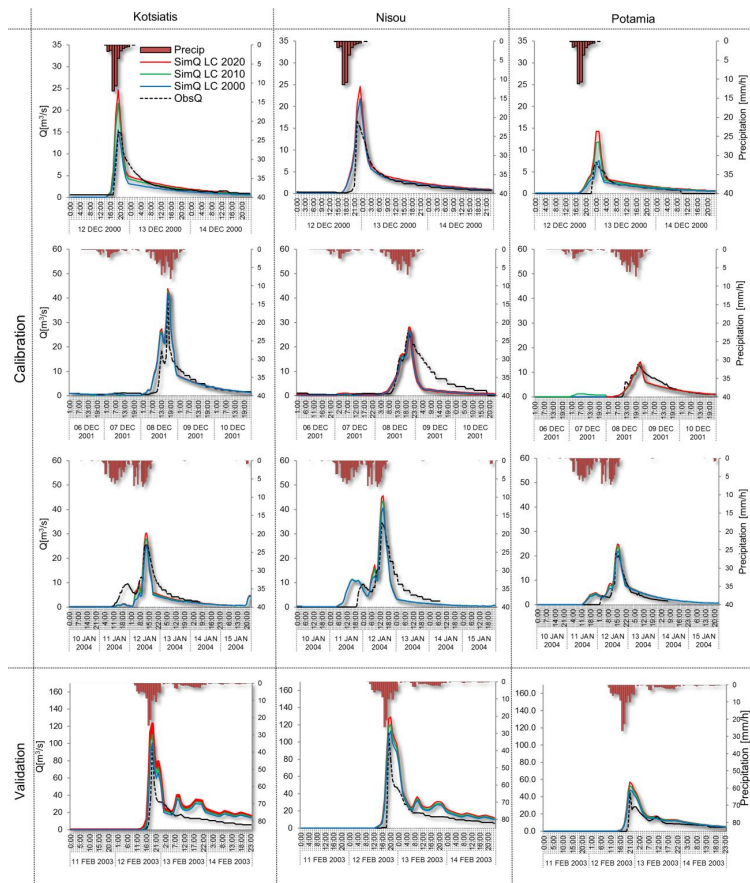


Fig. 11. Same as Fig. 8, with the hydrographs of land use 2010 (green lines) and 2020 (red lines) to be added.